

MASTER

One Dimensional Burn Computations for RFPR*

by

R. A. Nebel and G. H. Miley
Fusion Studies Laboratory
University of Illinois

R. W. Moses and R. L. Hagenson
Los Alamos Scientific Laboratory

I. Introduction

Previous studies¹ of the Reversed Field Pinch Reactor (RFPR) have been done with a zero-dimensional or "point-properties" formulation which averages all plasma profiles over the radius. In order to allow a closer examination of the RFPR performance and explore other phenomena, a more realistic one-dimensional (radial) plasma model (RFPBRN) has been developed² and applied to RFPR.

The earlier global model assumes flat temperature profiles, classical particle confinement, and magnetic field profiles determined through a pressure balance model alone. In contrast, the one-dimensional model determines the temperature and field profiles self-consistently and allows for instability induced transport as well. It also checks the plasma profiles' local and global stability characteristics. A major objective of this study was to determine how these additional physical effects would influence the RFPR design. Also, this new code allowed a more detailed optimization of the RFPR. Both aspects of the study are discussed here.

II. The Model

RFPBRN is a three fluid (ions, electrons, and alphas) one-dimensional, Lagrangian mesh transport and stability code. A quasi-static assumption is used so the plasma evolution can be followed on a resistive time scale. Linear ideal MHD stability is then periodically monitored as the profiles evolve in time.

*Supported by DOE Contracts DE-AS02-76ET52040 and W-7405-ENG-36

DISCLAIMER
The data presented herein were prepared by an officer of the United States Government. The data are not to be used for any other purpose than that for which they were prepared. The data are not to be used for any other purpose than that for which they were prepared. The data are not to be used for any other purpose than that for which they were prepared.

104

DISCLAIMER

This report was prepared as an account of work sponsored by an agency of the United States Government. Neither the United States Government nor any agency Thereof, nor any of their employees, makes any warranty, express or implied, or assumes any legal liability or responsibility for the accuracy, completeness, or usefulness of any information, apparatus, product, or process disclosed, or represents that its use would not infringe privately owned rights. Reference herein to any specific commercial product, process, or service by trade name, trademark, manufacturer, or otherwise does not necessarily constitute or imply its endorsement, recommendation, or favoring by the United States Government or any agency thereof. The views and opinions of authors expressed herein do not necessarily state or reflect those of the United States Government or any agency thereof.

DISCLAIMER

Portions of this document may be illegible in electronic image products. Images are produced from the best available original document.

The solution is found by integrating the temperature, density, and field profiles forward in time and then adiabatically readjusting the mesh to satisfy pressure balance. A variable time step predictor-corrector numeric technique is used to solve the diffusion section. The degree of implicitness for the numerics is controlled externally.

Transport coefficients are assumed to scale classically³ except for thermal conduction which, based on a review of data from Zeta experiments, is taken to be $\sim 1/200$ th Bohm. The perpendicular resistivity also assumes Bohm-like scaling in regions where Suydam's stability criterion⁴ is violated. The modeling in these regions is that of Christiansen and Roberts⁵.

MHD stability is monitored for both global and local modes. Local stability is monitored using Suydam's criterion while gross modes are checked using Newcomb's form of the ideal MHD energy principle⁵. The energy principle is minimized directly by using a Rayleigh-Ritz trial function expansion with arbitrary coefficients. The technique has the advantage that it shows whether the plasma is unstable to modes with wide (non-localized) eigenfunctions as well as determining the plasma's absolute stability characteristics.

III. Results

A. Zero-Dimensional and One-Dimensional Comparison

In order to match the global model as close as possible, the plasma edge was required to be the reversal point and the radius varied as:

$$r_p(t) = r_p(t=0) / \sqrt{1 - \beta_\theta(t)} \quad (1)$$

Initial conditions for temperature, density and field profiles were also taken consistent with the global model's pressure balance assumptions⁶.

Results generally showed similar trends, the principle difference being that the 1-D code ignited faster, burned out quicker, and had lower

fractional burnup (see Fig. 1). All of these features can be attributed to profile effects. The lower burnup resulted in an overall reduction in the energy gain factor Q_p to about 3/5's of that predicted by the 0-D code. While this is a significant difference, the agreement is still considered "good" in view of the many differences between the two codes (See Table I).

Inclusion of Suydam induced turbulent transport flattened the density profiles but had little effect on plasma performance. The reason this effect was small is that the stable outer region provided confinement while the Suydam induced energy transport was already dominated by the assumed Bohm-like thermal conductivity (See Table II).

B. Optimized Burn

In view of the reduced energy gain predicted by the 1-D model, a decision was made to use it to optimize Q_p . The density was raised to increase the power level near the global simulation parameters. The toroidal and poloidal fields were then reduced to the marginal amount required to ignite the plasma. Poloidal β and global stability were checked to see if the plasma maintained stability (which it did).

The results of the optimization are shown in Table I where it is seen that Q_p was increased by a factor of two. The principle reason that Q_p was doubled is that the radially varying temperature profile allows ignition on the magnetic axis which then propagates radially through the plasma. This allows the current (magnetic field energy) required for ignition to be lower which in turn raises Q_p .

Summary

Studies of the RFPR have been done using a one-dimensional three fluid transport and stability code. Results have verified trends predicted by

previous global studies. However, inclusion of profile effects, principally centerline ignition, has enabled the RFPR design to be optimized to obtain Q_p 's as high as 20. Assuming classical parallel resistivity, global MHD stability can be maintained throughout the entire burn.

References

1. R. L. Hagenson, R. A. Krakowski, and G. E. Cort, "The Reversed-Field Pinch Reactor," Los Alamos report LA-7973-MS (1979).
2. R. A. Nebel, et al., "Comparison of Zero-Dimensional and One Dimensional Thermonuclear Burn Calculations for the Reversed Field Pinch Reactor (RFPR)," Los Alamos report LA-8185-MS (1980).
3. S. I. Braginskii, Reviews of Plasma Physics, (Edited by M. A. Leontovich, Consultants Bureau, New York (1965)), 1, 205-311.
4. B. R. Suydam, "Stability of a Linear Pinch," P 1354, USA (1958).
5. J. P. Christiansen and K. V. Roberts, Nuclear Fusion, 18, 181-197, 2 (1978).
6. R. L. Hagenson, "Preliminary Physics and Engineering Considerations for a Fusion Power Plant Based on Reversed-Field Z-Pinch (RFZP) Confinement," Los Alamos Report LA-UR-76-2190 (1976).

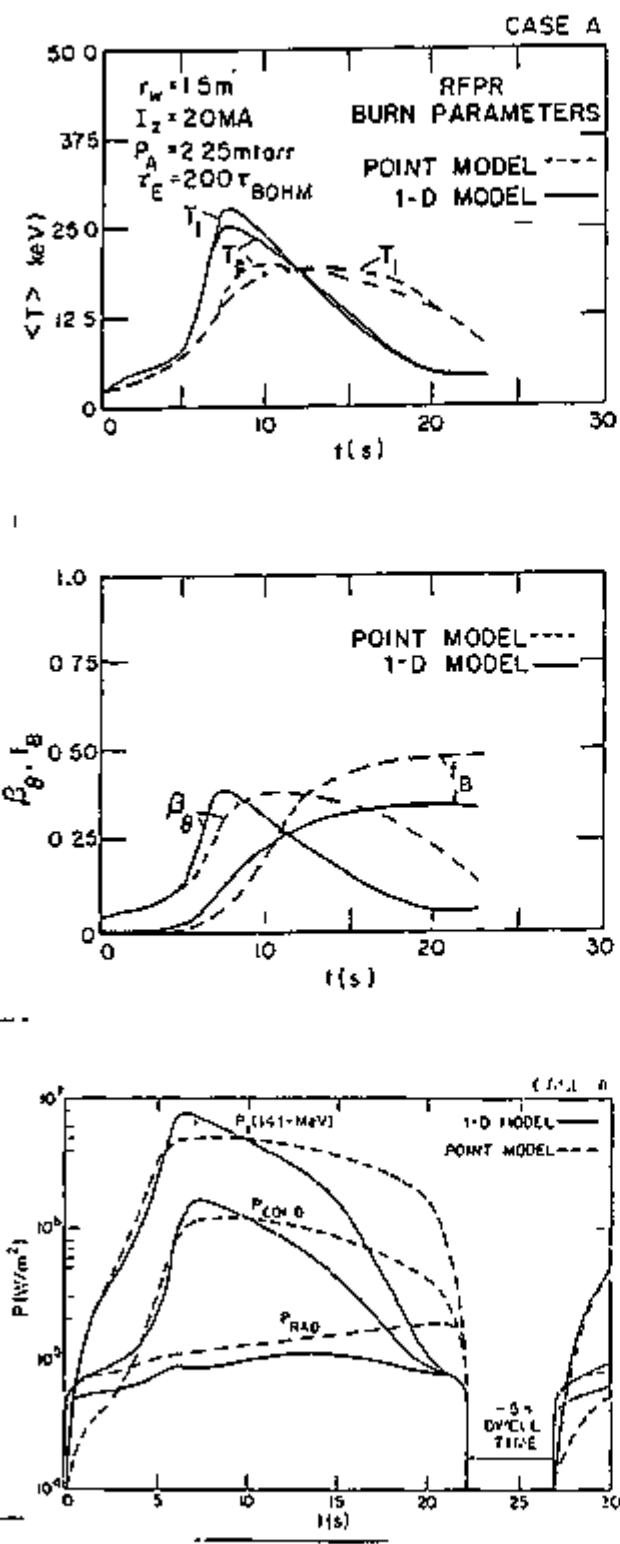


Table 1 Comparison of Energy Balance for Zero- and One-Dimensional Burn Models

PARAMETER (J/s)	1-D	0-D CASE A	0-D CASE B (OPTIMIZED)
Burn time t_b (s)	21.6	21.6	22.0
Initial plasma energy, W_{pi}	0.00	0.7	99
Final plasma energy, W_{pf}	2.5	1.9	1.60
Radiation energy, W_{RAD}	20.1	14.3	19.3
Ohmic heating energy, W_{OH}	7.1	6.5	6.91
Plasma energy loss (conduction), W_{CD}	117.5	93.0	146.7
Plasma expansion energy, W_{PE}	0.7	1.1	0.0
Magnetic field energy inside vessel wall at end of burn cycle, W_{BF}	51.0	45.0	30.6
Fusion neutron energy, W_f (14.1 MeV)	675.5	410.0	600.0
Q_p (fusion energy)/(ohmic + field energy)	-	9.3	20.0

^aradius forced to follow one-dimensional case
^bfixed plus a radius, Ohm conduction

Table 2 Comparison of Energy Balance for Nonuniform and Turbulent Transport

PARAMETER (J/s)	0-D ^a CASE B	0-D ^b CASE C
Burn time t_b (s)	24.0	25.0
Initial plasma energy, W_{pi}	0.3	0.5
Final plasma energy, W_{pf}	3.0	3.1
Radiation energy, W_{RAD}	14.4	13.5
Ohmic heating energy, W_{OH}	10.4	12.4
Plasma energy loss (conduction), W_{CD}	115.2	114.3
Plasma expansion energy, W_{PE}	0.0	0.0
Magnetic field energy inside first wall at end of burn cycle, W_{BF}	43.1	45.5
Fusion neutron energy, W_f (14.1 MeV)	-	675.5
Q_p (fusion energy)/(ohmic + field energy)	11.1	10.1

^afixed plasma radius, no Suydam turbulence
^bfixed plasma radius, Suydam turbulence